Decentralized Economic Dispatch in Microgrids via Heterogeneous Wireless Networks

Hao Liang, *Student Member, IEEE*, Bong Jun Choi, *Member, IEEE*, Atef Abdrabou, *Member, IEEE*, Weihua Zhuang, *Fellow, IEEE*, and Xuemin (Sherman) Shen, *Fellow, IEEE*

***Abstract*—As essential building blocks of the future smart grid, microgrids can efficiently integrate various types of distributed generation (DG) units to supply the electric loads at the minimum cost based on the economic dispatch. In this paper, we introduce a decentralized economic dispatch approach such that the optimal decision on power generation is made by each DG unit locally without a central controller. The prerequisite power generation and load information for decision making is discovered by each DG unit via a multiagent coordination with guaranteed convergence. To avoid a slow convergence speed which potentially increases the generation cost because of the time-varying nature of DG output, we present a heterogeneous wireless network architecture for microgrids. Low-cost short-range wireless communication devices are used to establish an ad hoc network as a basic information exchange infrastructure, while auxiliary dual-mode devices with cellular communication capabilities are optionally activated to improve the convergence speed. Two multiagent coordination schemes are proposed for the single-stage and hierarchical operation modes, respectively. The optimal number of activated cellular communication devices is obtained based on the tradeoff between communication and generation costs. The performance of the proposed schemes is analyzed and evaluated based on real power generation and load data collected from the Waterloo Region in Canada. Numerical results indicate that our proposed schemes can better utilize the cellular communication links and achieve a desired tradeoff between the communication and generation costs as compared with the existing schemes.**

***Index Terms*—Decentralized economic dispatch, heterogeneous wireless networks, microgrid, multiagent coordination.**

I. Introduction

OPERATING at a distribution voltage level, the microgrids are small-scale power systems designed to utilize the distributed generation (DG) units to supply the electrical loads in local areas such as a residential community, a university, and an industrial site [1]. In addition to the environmental benefit in terms of using more renewable energy sources, the microgrids can reduce the transmission and distribution (T&D) losses based on the physical proximity of DG units and loads. Since various types of DG units such as wind turbines, photovoltaic (PV) panels, and fuel cells may coexist, one pivotal problem in microgrid management is the economic dispatch which balances the power generation and loads at a minimum monetary cost. Different from traditional power systems with thermal energy power generators, the economic dispatch in microgrids is challenging because of the intermittent and climate-dependent nature of renewable energy sources. As the accuracy of estimating the capacity of DG units and loads is limited, the economic dispatch is performed in a relatively small time scale, e.g., every five minutes for California Independent System Operator (CAISO) with wind/solar integration [2], and a communications/control delay within 2-10 seconds [3].

Both centralized and decentralized approaches can be used to achieve economic dispatch. Most existing centralized approaches assume that the estimates or statistics of power generation and loads acquired by a central controller are accurate [4], [5], [6]. Although the centralized economic dispatch has the advantage of high efficiency, it suffers from the problem of a single point of failure and high deployment cost in terms of a powerful central controller and a communication infrastructure (such as a fiber-optic network [1] to connect each DG unit or load to the central controller). On the other hand, the decentralized economic dispatch can avoid a single point of failure and fits the plug-and-play nature of DG units and loads in microgrids [7]. Since information exchange only needs to be established among neighboring nodes (corresponding to the DG units or loads), low-cost short-range wireless communication devices such as WiFi and ZigBee devices can be implemented to establish the network infrastructure [8]. In order to achieve the same efficiency in cost minimization as the centralized counterpart, the DG units should acquire the accurate power generation and load information in a decentralized manner [9]. Multiagent coordination is a promising solution for decentralized load restoration [10] in microgrids since the accuracy of information discovery is guaranteed based on the average consensus theory. Several medium access control (MAC) protocols are proposed in [11] to facilitate multiagent coordination in microgrids via wireless networks. However, as the convergence speed decreases significantly as the network size increases, how to implement multiagent coordination to achieve economic dispatch in a small time scale is still an open issue. Although better network connectivity can improve the convergence speed of multiagent coordination according to the small-world phenomenon [12], simply increasing the transmission power of wireless devices is not helpful since the connectivity benefit is reduced by increased wireless interference [13]. Therefore, an auxiliary network infrastructure is indispensable for efficient decentralized economic dispatch in microgrids via wireless networks.

Manuscript received 1 October 2011; revised 14 February 2012.
H. Liang, B. J. Choi, W. Zhuang, and X. Shen are with the Department of Electrical and Computer Engineering, University of Waterloo, 200 University Avenue West, Waterloo, Ontario, Canada N2L 3G1 (e-mail: {h8liang, bjchoi, wzhuang, sshen}@uwaterloo.ca).
A. Abdrabou is with the Department of Electrical Engineering, UAE University, Al-Ain, Abu Dhabi, 17555, UAE (e-mail: atef.abdrabou@uaeu.ac.ae).
Digital Object Identifier 10.1109/JSAC.2012.120705.

TABLE I
SUMMARY OF IMPORTANT SYMBOLS USED.

Symbols	Definitions
$\mathcal{B}$	The set of dual-mode nodes
$\mathbf{c}$	The set of all possible costs in economic dispatch
G	The number of types of DG units
$\mathcal{M}$ (M)	The set (number) of activated cellular communication devices
$\mathcal{N}_v$	The set of neighboring nodes of node v
$\mathcal{Q}_m$	The set of cluster members with respect to node m
$S_{\mathcal{Q}_m}$	The number of time slots for deterministic ad hoc communication link scheduling with respect to the nodes in $\mathcal{Q}_m$
T	The duration of information exchange period
T_A	The duration of information exchange via ad hoc network for hierarchical multiagent coordination
T_B	The duration of one broadcast
T_D	The duration of economic dispatch period
$\mathcal{V}$	The set of all nodes in the microgrid
X_g $(\bar{X}_g)$	The (average) cumulative capacity of type g DG units
Y $(\bar{Y})$	The (average) aggregated loads

In this paper, we present a heterogeneous wireless network architecture to achieve decentralized economic dispatch in microgrids. Each node is equipped with a short-range (e.g., WiFi or ZigBee) wireless communication device for information exchange in an ad hoc mode. Several nodes are further equipped with cellular communication devices and are referred to as dual-mode nodes for connectivity improvement. By activating the cellular communication devices, information exchange beyond the one-hop neighbors in the ad hoc network can be enabled. Based on the analysis of the economic dispatch problem, an equivalence between the optimal economic dispatch and average consensus is shown. A multiagent coordination approach is proposed to solve the economic dispatch problem such that each node only needs to discover the average values of the cumulative capacity (i.e., the maximum aggregated output) of each type of DG units and aggregated loads. To avoid a slow convergence speed of multiagent coordination, the cellular communication devices of the dual-mode nodes are optionally activated. Two multiagent coordination schemes are proposed to incorporate the cellular communication links. The single-stage multiagent coordination scheme requires only neighboring node information and is fully distributed, while the hierarchical multiagent coordination scheme utilizes the network topology information for performance improvement based on clustering and deterministic wireless link scheduling. The convergence speeds of both schemes are analyzed with respect to the number of activated cellular communication devices. The analytical results show that, with more cellular communication devices being activated, a (possible) improvement in the convergence speed can be obtained.

Although the ad hoc network based on WiFi or ZigBee devices can operate on the license-free industrial, scientific and medical (ISM) band without monetary cost for radio spectrum, the cost of using cellular communication devices is comparable to the incremental generation cost caused by packet delay and packet losses [14] [15]. For economic dispatch in microgrids which addresses the cost minimization issues, a tradeoff between the communication and power generation costs is indispensable. In this paper, we focus on the network operation cost in terms of data transmission via cellular network and the incremental generation cost incurred by the error in multiagent coordination, and formulate an optimization problem for the tradeoff. Based on an approximation of the incremental generation cost with respect to the undelivered and extra power in a microgrid, we show that a desired tradeoff can be achieved without resorting to the accurate knowledge of power generation and load statistics. The performance of the proposed schemes is evaluated based on real power generation and load data collected from Waterloo Region in Canada. To the best of our knowledge, this is the first work in literature to address the decentralized economic dispatch in microgrids via multiagent coordination and to present a heterogeneous wireless network architecture for better tradeoff between the communication and generation costs. The significance of this research is threefold. From the utilities' point of view, the economic dispatch in microgrids can be achieved based on wireless communication devices at a low deployment cost and the minimum operation cost. From the environmental point of view, the use of traditional thermal energy power generators can be reduced via a better utilization of the renewable energy sources. At the same time, the customers can enjoy the monetary benefit in terms of reduced electricity bills which, in turn, promotes the use of the renewable energy sources.

The remainder of this paper is organized as follows. Section II describes the system model. Section III presents the proposed decentralized economic dispatch approach based on multiagent coordination. The proposed single-stage and hierarchical multiagent coordination schemes are presented in Section IV and Section V, respectively. The tradeoff between the communication and generation costs is investigated in Section VI. Numerical results are given in Section VII. Section VIII concludes the paper and identifies future research

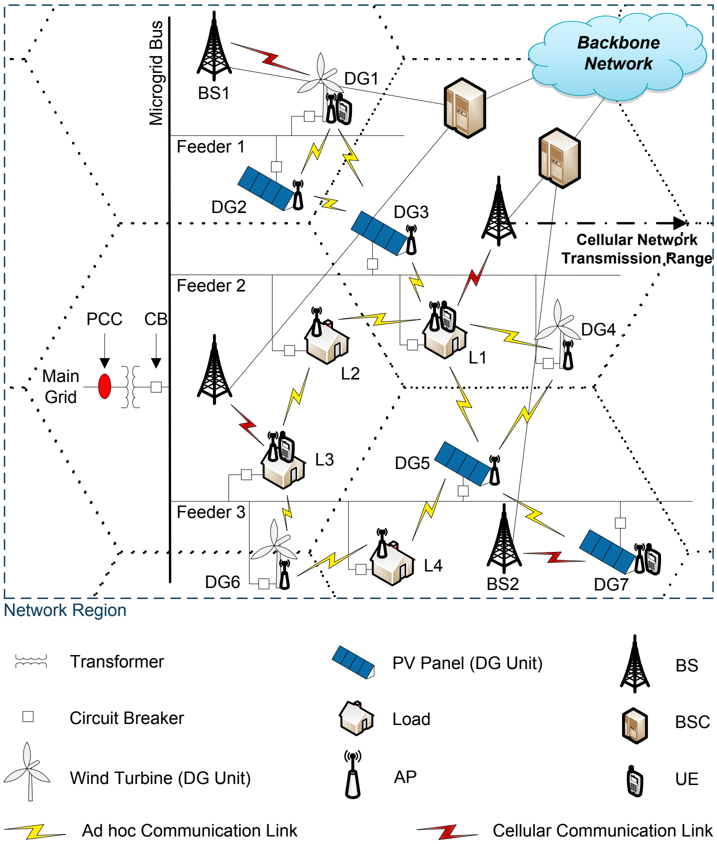

Fig. 1. An illustration of the microgrid configuration with a heterogeneous wireless network infrastructure.

topics. As many symbols are used in this paper, Table I summarizes the important ones.

II. System Model

As shown in Fig. 1, we consider a microgrid built for a small residential community. Electric power is delivered from the DG units (i.e., the wind turbines and PV panels) to the loads (i.e., the residential houses) via the power grid infrastructure. The power generation and loads are balanced via economic dispatch every T_D (hour), where $T_D < 1$ for renewable energy source integration [2]. The information exchange for the economic dispatch is based on a heterogeneous wireless network infrastructure[1] and is completed at the beginning of each economic dispatch period with a short duration T ($T < T_D$) [3], as shown in Fig. 2(a). In the following, we consider one economic dispatch period as an example. Each DG unit or load is represented by a node in the microgrid. The set of all nodes in the microgrid is denoted as $\mathcal{V}$ and is indexed by $1, 2, \cdots, |\mathcal{V}|$.

A. Microgrid and Electricity Pricing

The microgrid is connected to the main grid (i.e., the utility grid) via a point of common coupling (PCC) [1]. The microgrid can operate either in a grid-connected mode or an islanded mode, by closing or opening the circuit breaker (CB) between the PCC and microgrid bus, respectively. Without loss of generality, we consider an islanded mode in this paper with an opened CB. An example of the microgrid is shown in Fig. 1. There are three feeders in the microgrid. On feeder 1, there are two DG units (DG1 and DG2). On feeder 2, there are two loads (L1 and L2) and two DG units (DG3 and DG4). On feeder 3, there are two loads (L3 and L4) and three DG units (DG5, DG6, and DG7).

Suppose there are G types of DG units in the microgrid. For each node v ($v \in \mathcal{V}$), its type g ($g \in \{1, 2, \cdots, G\}$) power generation capacity is given by x_{gv}. Specifically, we have $x_{gv} > 0$ if node v is a DG unit and belongs to type g, and $x_{gv} = 0$ otherwise. Take wind turbine as an example, the value of x_{gv} is equal to the maximum output of the wind turbine given the wind speed during the economic dispatch period. Similarly, let y_v denote the power demand of each node with $y_v > 0$ if node v represents a load and $y_v = 0$ otherwise. Note that we use the generalized definitions of x_{gv} and y_v for all nodes in $\mathcal{V}$ for notation clarity. Denote $\mathbf{x} = \{x_{gv} | g \in \{1, 2, \cdots, G\}, v \in \mathcal{V}\}$ and $\mathbf{y} = \{y_v | v \in \mathcal{V}\}$ as the sets of power generation capacity and loads, respectively. The values of $\mathbf{x}$ and $\mathbf{y}$ are assumed to be constant within each economic dispatch period[2] and vary randomly among different periods.

In this work, we consider a linear generation cost model which is widely used for the integration of DG units such as

[1]The power supply of the network infrastructure is considered to be independent of the microgrid since the supervisory control should be uninterruptible even when fault occurs in the power grid [10].

[2]According to experimental results, there is typically a 3%-5% relative error for wind farm power estimation in a 10-minute interval [16].

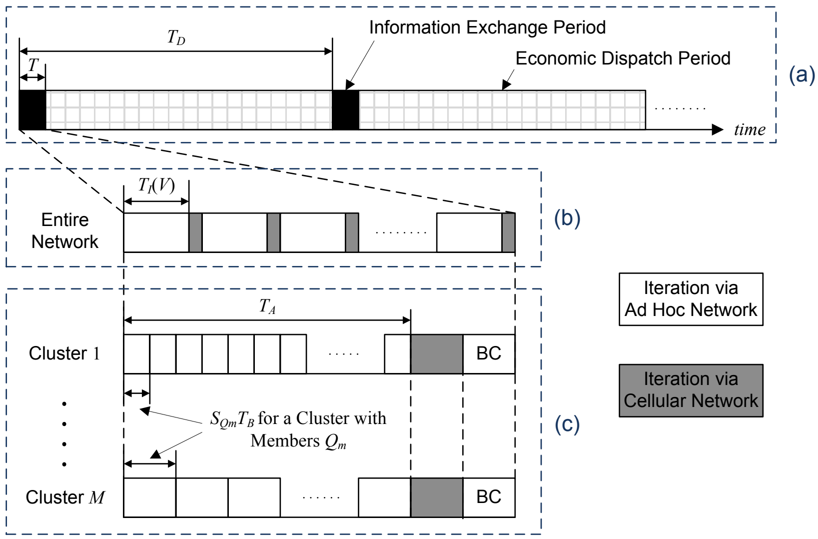

Fig. 2. Economic dispatch and multiagent coordination: (a) Period definition. (b) Single-stage multiagent coordination. (c) Hierarchical multiagent coordination.

the one used by the feed-in tariff (FIT) program of Ontario Power Authority [17]. The cost of unit power generation of type g DG unit is denoted as c_g (in dollar/kWh). Without loss of generality, we consider ordered costs, i.e., $0 < c_1 \leq c_2 \leq \cdots \leq c_G$. For instance, the solar energy is more expensive than wind or hydro energy according to the FIT program. The economic dispatch in a microgrid aims at balancing the power generation and loads at a minimum cost. For simplicity, we do not consider the power flow limit of the feeders and the power losses in the microgrid. However, because of the uncertainty in DG output and/or the error in information discovery, the power generation and loads may not be balanced perfectly. Specifically, if the power generation of DG units is not enough to supply the loads, the undelivered power should be purchased from alternative sources such as traditional thermal energy power generators at a cost of c_A per unit. On the other hand, the extra power in the microgrid is compensated by negative spinning reserves at a cost of c_E per unit[3]. Generally, we have $c_A > c_G$ and $c_E \geq 0$. The set of all possible costs in economic dispatch is denoted as $\mathbf{c} = \{c_g | g \in \{1, 2, \cdots, G\}\} \cup \{c_A, c_E\}$ and is assumed to be constant for the time frame under consideration.

B. Heterogeneous Wireless Networks

Each node in $\mathcal{V}$ is equipped with a short-range wireless communication device, such as the access point (AP) of a WiFi or ZigBee based device[4]. Multi-channel wireless communication is supported. For instance, we have 23 wireless channels for IEEE 802.11a based WiFi devises and 16 wireless channels for IEEE 802.15.4 based ZigBee devices. Because of a limited wireless transmission range, each node can only communicate with (or cause interference to) its one-hop neighbors operating on the same channel. For instance, in Fig. 1, the node corresponding to DG5 can communicate with the nodes corresponding to L1, L4, DG4, and DG7, given that they operate on the same channel. Concurrent transmissions over the non-overlapping channels are considered interference free. We denote the network based on the short-range wireless communication devices as an ad hoc network and the set of neighbors of node v ($v \in \mathcal{V}$) as $\mathcal{N}_v$ ($\mathcal{N}_v \subseteq \mathcal{V} \setminus \{v\}$). The wireless devices have a constant transmission rate and a transmission range equal to the interference range. Specifically, a transmission of node v can interfere with another transmission to node n only if $n \in \mathcal{N}_v$, which results in an unsuccessful reception at node n. For the ad hoc network, there exists a (multi-hop) communication path between any pair of two nodes. In other words, the ad hoc network is strongly connected.

A subset $\mathcal{B}$ ($\mathcal{B} \subseteq \mathcal{V}$) of nodes are further equipped with cellular communication devices, such as the user equipments (UEs) in a universal mobile telecommunications system (UMTS) [22]. Since the base stations (BSs) of the cellular network are connected by the base station controllers (BSCs) and are further connected to a backbone network, the $\mathcal{B}$ nodes can communicate with each other even if they are not one-hop neighbors in the ad hoc network. For instance, in Fig. 1, DG1, DG7, L1, and L3 can communicate with each other. For simplicity, we neglect the delay of information exchange via a cellular network which can support services with stringent delay requirements [23], [24], [25]. The cost of sending a message from one node to another via the cellular network is c_M, which depends on the size of the data message.

III. Decentralized Economic Dispatch based on Multiagent Coordination

In this section, we first analyze the economic dispatch problem and show that solving the economic dispatch problem is equivalent to achieving average consensus in the microgrid. Then, we propose a decentralized economic dispatch approach

[3]If the service is purchased before real-time operation, an estimation of the maximum extra power is required. The energy waste can be reduced based on distributed energy storage systems [1] and vehicle-to-grid systems [19], [20], [18], which is left for our future research.

[4]An extension to power line communications (PLC) is straightforward since the PLC channel is interference limited and the transmission range of PLC devices is limited in general [10][21].

where each node makes a local decision on power generation based on the average values of the cumulative capacity of each type of DG units and the aggregated loads. The information required for decision making is discovered by each node via multiagent coordination with guaranteed convergence.

A. Economic Dispatch

The economic dispatch in a microgrid schedules the power generation (or output) of DG units optimally such that the electric loads are served at a minimum cost. Denote the power generation of a type g DG unit v as u_{gv} ($0 \leq u_{gv} \leq x_{gv}$). The total generation cost (in dollar/h) equals the cost of purchasing power from the DG units and alternative energy sources plus the cost of purchasing negative spinning reserves, given by

$$C_P(\mathbf{x}, \mathbf{y}, \mathbf{c}, \mathbf{u}) = \sum_{g \in \{1,2,\cdots,G\}} \sum_{v \in \mathcal{V}} c_g u_{gv} + c_A z_A + c_E z_E \quad (1)$$

where z_A and z_E denote the undelivered power which should be purchased from the alternative sources and the extra power, respectively. Denote $\mathbf{u} = \{u_{gv} | g \in \{1,2,\cdots,G\}, v \in \mathcal{V}\}$ as a specific policy of economic dispatch. Based on the power balance (or demand-supply balance) equation [4], we have $z_A = \left(\sum_{v \in \mathcal{V}} y_v - \sum_{g \in \{1,2,\cdots,G\}} \sum_{v \in \mathcal{V}} u_{gv}\right)^+$ and $z_E = \left(\sum_{g \in \{1,2,\cdots,G\}} \sum_{v \in \mathcal{V}} u_{gv} - \sum_{v \in \mathcal{V}} y_v\right)^+$. Then, the optimal economic dispatch policy $\mathbf{u}^*$ is determined by problem P1 as

$$(\mathbf{P1}) \ \min_{\mathbf{u}} \ C_P(\mathbf{x}, \mathbf{y}, \mathbf{c}, \mathbf{u}) \quad (2)$$

$$\text{subject to} \ \ 0 \leq u_{gv} \leq x_{gv}, \ g \in \{1,2,\cdots,G\}, v \in \mathcal{V}. \quad (3)$$

Accordingly, we denote the minimum generation cost based on $\mathbf{u}^*$ as $C_P^*(\mathbf{x}, \mathbf{y}, \mathbf{c}) = C_P(\mathbf{x}, \mathbf{y}, \mathbf{c}, \mathbf{u}^*)$.

B. Optimal Economic Dispatch and Average Consensus

In general, problem P1 is a linear programming (LP) problem which can be solved by existing methods. However, in order to solve problem P1 in a decentralized manner, the values of all elements in $\mathbf{x}$ and $\mathbf{y}$ should be obtained by each node, which results in a high communication overhead. In this subsection, we derive a closed-form expression of the optimal economic dispatch policy based on the ordered generation costs. The information required by each node for decentralized decision making is reduced to the average values of the cumulative capacity of each type of DG units and the aggregated loads.

We first have the following two lemmas with respect to the extra and undelivered power in a microgrid. The proofs of both lemmas are based on contradiction and are omitted here because of space limitation.

Lemma 1. *For an optimal economic dispatch policy $\mathbf{u}^* = \{u_{gv}^* | g \in \{1,2,\cdots,G\}, v \in \mathcal{V}\}$ based on problem P1, there is no extra power in the microgrid, i.e., $z_E^* = 0$.*

Lemma 2. *If $\sum_{g \in \{1,2,\cdots,G\}} \sum_{v \in \mathcal{V}} x_{gv} > \sum_{v \in \mathcal{V}} y_v$, there is no undelivered power, i.e., $z_A^* = 0$. Taking account of Lemma 1, we have $\sum_{g \in \{1,2,\cdots,G\}} \sum_{v \in \mathcal{V}} u_{gv}^* = \sum_{v \in \mathcal{V}} y_v$, i.e., the optimal aggregated power generation of the G types of DG units and the aggregated loads are balanced in a microgrid.*

Denote the cumulative capacity of the DG units and the aggregated loads as $\mathbf{X} = \{X_g | g \in \{1,2,\cdots,G\}\}$ and $Y = \sum_{v \in \mathcal{V}} y_v$, respectively, where $X_g = \sum_{v \in \mathcal{V}} x_{gv}$ represents the cumulative capacity of type g DG units. Define an economic dispatch policy as follows:

$$u_{gv}(\bar{\mathbf{X}}, \bar{Y}, \mathbf{c}) = \begin{cases} x_{gv}, & \text{if } \bar{Y} \geq \sum_{k \in \{1,2,\cdots,g\}} \bar{X}_k \\ 0, & \text{if } \bar{Y} \leq \sum_{k \in \{1,2,\cdots,g-1\}} \bar{X}_k \\ \frac{x_{gv}}{\bar{X}_g} \left[\bar{Y} - \sum_{k \in \{1,2,\cdots,g-1\}} \bar{X}_k\right], & \text{elsewhere} \end{cases} \quad (4)$$

where $\bar{\mathbf{X}} = \{\bar{X}_g | g \in \{1,2,\cdots,G\}\}$, $\bar{X}_g = X_g / |\mathcal{V}|$ and $\bar{Y} = Y / |\mathcal{V}|$ are the average values of cumulative capacity and aggregated loads, respectively. For the third case in (4), the power generation of the DG units is proportional to their capacity, also known as the proportional fairness. Then, we have the following theorem which is proved in Appendix.

Theorem 1. *Given the average values of the cumulative capacity $\bar{\mathbf{X}}$ and aggregated loads $\bar{Y}$, the decentralized economic dispatch policy in (4) is optimal for problem P1.*

Based on Theorem 1, the problem of decentralized economic dispatch is transformed into the discovery (by each node) of the the average values of the cumulative capacity ($\bar{X}_g$) of each type of DG units and aggregated loads ($\bar{Y}$). Intuitively, the results follow the power balance equation which is based on the summation of power generation and/or loads. In this work, we consider a multiagent coordination scheme since the convergence of information discovery can be guaranteed based on the average consensus theory.

C. Multiagent Coordination via Ad Hoc Network

In this subsection, we investigate the multiagent coordination via the ad hoc network and show the convergence of the information discovery process. Take the discovery of the average cumulative capacity of type g DG units ($\bar{X}_g$) as an example. The information update takes place in a discrete-time manner, where each round of update is referred to as an iteration. Suppose the iterations are completed at time steps t_k ($k \in \{0,1,2,\cdots\}$) with $t_0 = 0 < t_1 < t_2 < \cdots \leq T$. Denote the state value kept by node v ($v \in \mathcal{V}$) at time t_k as $\bar{X}_g(v, t_k)$. For the initial value, we have $\bar{X}_g(v, t_0) = x_{gv}$. For the kth iteration, node v ($v \in \mathcal{V}$) acquires the state values $\bar{X}_g(n, t_{k-1})$ ($n \in \mathcal{N}_v$) kept by its neighboring nodes via ad hoc communication links. Then, the state value kept by node v is updated based on a weighted average of the acquired values, given by

$$\bar{X}_g(v, t_k) = \sum_{n \in \mathcal{V}} \omega_{\mathcal{V}}^a(v, n) \bar{X}_g(n, t_{k-1}) \quad (5)$$

where $\omega_{\mathcal{V}}^a(v, n) \geq 0$ is the weight used by node v with respect to node n. Here, we study a symmetric version of the natural random walk [13] which is analytically tractable. The weight values are given by

$$\omega_{\mathcal{V}}^a(v, n) = \begin{cases} \frac{1}{2\max\{|\mathcal{N}_v|, |\mathcal{N}_n|\}}, & \text{if } n \in \mathcal{N}_v \\ 1 - \sum_{j \in \mathcal{N}_v} \frac{1}{2\max\{|\mathcal{N}_v|, |\mathcal{N}_j|\}}, & \text{if } n = v \\ 0, & \text{elsewhere.} \end{cases} \quad (6)$$

Based on (6), we have $\omega^a_{\mathcal{V}}(v,n) > 0$ if $n \in \mathcal{N}_v \cup \{v\}$ and $\omega^a_{\mathcal{V}}(v,n) = 0$ otherwise. The update in (5) is fully decentralized such that each node only needs the information from its direct neighbors. Denote the weight matrix of each iteration as $W^a_{\mathcal{V}} = [\omega^a_{\mathcal{V}}(v,n)]_{|\mathcal{V}|\times|\mathcal{V}|}$, we have

$$\bar{X}_{g,\mathcal{V}}(t_k) = W^a_{\mathcal{V}} \bar{X}_{g,\mathcal{V}}(t_{k-1}) \tag{7}$$

where $\bar{X}_{g,\mathcal{V}}(t_k) = (\bar{X}_g(1,t_k), \cdots, \bar{X}_g(|\mathcal{V}|,t_k))^\top$. The wireless links for each iteration may be scheduled sequentially to avoid interference since we may have $\mathcal{N}_v \cap \mathcal{N}_j \neq \emptyset$ for some $v, j \in \mathcal{V}$.

Define a directed graph associated with $W^a_{\mathcal{V}}$ such that the vertex set is $\mathcal{V}$ and there is an edge from vertex i to vertex j $(i,j \in \mathcal{V})$ if and only if $\omega^a_{\mathcal{V}}(i,j) > 0$. Since $W^a_{\mathcal{V}}$ is doubly stochastic and the directed graph associated with $W^a_{\mathcal{V}}$ is strongly connected (based on the assumption that the ad hoc network is strongly connected), the state value of each node converges to a constant [26][27], given by

$$\lim_{t\to\infty} \bar{X}_g(v,t) = \bar{X}_g, \ v \in \mathcal{V}. \tag{8}$$

In other words, all nodes in the network can eventually obtain the same state value on the average cumulative capacity of type g DG units. Similarly, we can show the convergence of the state values with respect to the average aggregated loads $\bar{Y}$ which is updated as

$$\bar{Y}_{\mathcal{V}}(t_k) = W^a_{\mathcal{V}} \bar{Y}_{\mathcal{V}}(t_{k-1}) \tag{9}$$

where $\bar{Y}_{\mathcal{V}}(t_k) = (\bar{Y}(1,t_k), \cdots, \bar{Y}(|\mathcal{V}|,t_k))^\top$.

The convergence of the multiagent coordination ensures that an accurate decentralized decision can be made by each node if T is sufficiently large. However, for the economic dispatch in a small time scale, the convergence should be reached in a short time. The error of multiagent coordination at time T is bounded by

$$||\Phi_{g,\mathcal{V}}(T)||_2 \le |\lambda_2(W^a_{\mathcal{V}})|^{\lfloor \frac{T}{T_I(\mathcal{V})} \rfloor} ||\Phi_{g,\mathcal{V}}(0)||_2 \tag{10}$$

where $\lambda_k(\cdot)$ represents the kth largest eigenvalue (in module), and $\Phi_{g,\mathcal{V}}(t)$ is the disagreement vector [27], given by

$$\begin{aligned} \Phi_{g,\mathcal{V}}(t) = \big(&\bar{X}_g(1,t) - \bar{X}_g, \bar{X}_g(2,t) - \bar{X}_g, \cdots, \\ &\bar{X}_g(|\mathcal{V}|,t) - \bar{X}_g\big)^\top . \end{aligned} \tag{11}$$

In (10), $T_I(\mathcal{V})$ is the duration of each iteration via the ad hoc network with respect to nodes in $\mathcal{V}$, which depends on the wireless link scheduling.

As the network size increases, the convergence speed of multiagent coordination in the ad hoc network decreases significantly [10] [13]. We propose to utilize the cellular communication links to improve network connectivity and thus the convergence speed according to the small-world phenomenon [12]. Denote $\mathcal{M}$ $(\mathcal{M} \subseteq \mathcal{B})$ as the set of dual-mode nodes for which the cellular communication devices are activated, where $M = |\mathcal{M}|$ $(M \ge 2)$ represents the number of activated cellular communication devices. In the next two sections, we present two multiagent coordination schemes to utilize both the ad hoc and cellular communication links.

IV. Single-Stage Multiagent Coordination

The single-stage multiagent coordination utilizes the cellular network to deliver information among the nodes in $\mathcal{M}$ after each iteration in the ad hoc network, as shown in Fig. 2(b). The single-stage multiagent coordination is fully decentralized such that the network topology information is not required. Given the value of M, the nodes in $\mathcal{M}$ are randomly selected. All nodes in $\mathcal{V}$ operate on the same frequency channel to ensure successful information exchanges via the ad hoc network.

A. Update-and-Continue based Random Access

For the information exchange via the ad hoc network, the wireless link access is random without requiring network topology information. Since multiagent coordination operates in a synchronous manner according to (5), after each update, node v should wait until the next iteration begins (i.e., all other nodes finish their current update) to guarantee the convergence. However, the time of each iteration (i.e., $T_I(\mathcal{V})$ in (10)) becomes a random variable because of the random access scheme. In order to avoid that each node waits for the worst-case iteration time (refereed to as the update-and-wait based random access scheme [10]), we consider an update-and-continue based random access scheme [11] such that each node starts to transmit the updated state values to its neighbors following the completion of its own update. The neighboring nodes store the received state values and use them for the next iteration following the completion of the current update. In order to implement the update-and-continue based random access, an index number is assigned to each iteration.

B. Iteration via Cellular Network

Since all cellular BSs are connected to a backbone network, we consider all nodes in $\mathcal{M}$ as direct neighbors of each other during the iteration via cellular network. An iteration via the cellular network includes the information exchange among each pair of nodes in $\mathcal{M}$. A uniform weight matrix [28] without the need of network topology information is used for the update of the state values, given by $W^c_{\mathcal{M}} = [\omega^c_{\mathcal{M}}(v,n)]_{|\mathcal{V}|\times|\mathcal{V}|}$, where $\omega^c_{\mathcal{M}}(v,n)$ is given by

$$\omega^c_{\mathcal{M}}(v,n) = \begin{cases} 1/M, & \text{if } v,n \in \mathcal{M} \\ 1, & \text{if } v,n \in \mathcal{V} \setminus \mathcal{M} \text{ and } v = n \\ 0, & \text{elsewhere} \end{cases} \tag{12}$$

where the second case corresponds to the ad hoc nodes or the dual-mode nodes with inactivated cellular communication devices. For an iteration via both the ad hoc and cellular networks, the weight matrix is given by $W^c_{\mathcal{M}} W^a_{\mathcal{V}}$, i.e.,

$$\bar{X}_{g,\mathcal{V}}(t_k) = W^c_{\mathcal{M}} W^a_{\mathcal{V}} \bar{X}_{g,\mathcal{V}}(t_{k-1}) \tag{13}$$

$$\bar{Y}_{\mathcal{V}}(t_k) = W^c_{\mathcal{M}} W^a_{\mathcal{V}} \bar{Y}_{\mathcal{V}}(t_{k-1}). \tag{14}$$

Since $W^c_{\mathcal{M}}$ is doubly stochastic, $W^c_{\mathcal{M}} W^a_{\mathcal{V}}$ is doubly stochastic. In the next section, we show that the graph associated with $W^c_{\mathcal{M}} W^a_{\mathcal{V}}$ is strongly connected. Therefore, the convergence of the single-stage multiagent coordination is guaranteed.

C. Performance Analysis

In this subsection, we analyze the benefit of using the cellular communication links to improve the convergence speed of multiagent coordination. According to (10), we focus on the second largest eigenvalue of the weight matrix. Consider a finite-state Markov chain with state space $\mathcal{V}$ and state transition matrix (or stochastic matrix) $W = [w(i,j)]_{|\mathcal{V}|\times|\mathcal{V}|}$[5]. Define the closed subset and irreducible closed subset as follows.

Definition 1. *A set $\mathcal{M}$ of states is a closed subset of a Markov chain with state transition matrix W if and only if $w(i,j)=0$ for any $i \in \mathcal{M}$ and $j \in \mathcal{V}\setminus\mathcal{M}$. A set $\mathcal{M}'$ of states is an irreducible closed subset if and only if $\mathcal{M}'$ is a closed subset, and no proper subset of $\mathcal{M}'$ is a closed subset.*

Then, the following lemma holds with respect to eigenvalues of the state transition matrix of a Markov chain [29].

Lemma 3. *The state transition matrix W has an eigenvalue 1, and the multiplicity of the eigenvalue 1 is equal to the number of irreducible closed subsets of the Markov chain.*

Based on Lemma 3, we have the following properties with respect to the weight matrices $W_{\mathcal{M}}^c$ and $W_{\mathcal{V}}^a$.

Lemma 4. *Both $W_{\mathcal{M}}^c$ and $W_{\mathcal{V}}^a$ are symmetric and positive semidefinite.*

Proof: According to the definitions of $W_{\mathcal{M}}^c$ and $W_{\mathcal{V}}^a$, we can easily verify that both matrices are symmetric. For the matrix $W_{\mathcal{M}}^c$, the states of the associated Markov chain can be partitioned into $|\mathcal{V}|-M+1$ irreducible closed subsets, i.e., $|\mathcal{V}|-M$ subsets correspond to the nodes with only short-range communication devices and the dual-mode nodes with inactivated cellular communication devices, and one subset corresponds to $\mathcal{M}$. According to Lemma 3, the eigenvalues of $W_{\mathcal{M}}^c$ include $|\mathcal{V}|-M+1$ ones. On the other hand, we can easily verify the rank of $W_{\mathcal{M}}^c$ is $|\mathcal{V}|-M+1$ since the weights used by all nodes in $\mathcal{M}$ are the same. Therefore, the other $M-1$ eigenvalues of $W_{\mathcal{M}}^c$ are equal to zero, which indicates that $W_{\mathcal{M}}^c$ is positive semidefinite.

For the matrix $W_{\mathcal{V}}^a$, the Laplacian of the associated graph is given by

$$L_{\mathcal{V}}^a = I - W_{\mathcal{V}}^a. \tag{15}$$

Since the Laplacian of the strongly connected graph is positive semidefinite [27], we have $\lambda_k(L_{\mathcal{V}}^a) \geq 0$ for all $k \in \{1,2,\cdots,|\mathcal{V}|\}$. Moreover, we have

$$\sum_{j\in\mathcal{N}_i}\omega_{\mathcal{V}}^a(i,j) = \sum_{j\in\mathcal{N}_i}\frac{1}{2\max\{|\mathcal{N}_i|,|\mathcal{N}_j|\}} \leq \frac{|\mathcal{N}_i|}{2|\mathcal{N}_i|} = \frac{1}{2} \tag{16}$$

where the inequality holds since $\max\{|\mathcal{N}_i|,|\mathcal{N}_j|\} \geq |\mathcal{N}_i|$. Therefore, the spectral radius of $L_{\mathcal{V}}^a$ is bounded as

$$\begin{aligned}\rho(L_{\mathcal{V}}^a) &\leq \max_{i\in\mathcal{V}}\{|-\sum_{j\in\mathcal{N}_i}\omega_{\mathcal{V}}^a(i,j)| + \sum_{j\in\mathcal{N}_i}|\omega_{\mathcal{V}}^a(i,j)|\}\\ &= 2\max_{i\in\mathcal{V}}\sum_{j\in\mathcal{N}_i}\omega_{\mathcal{V}}^a(i,j) \leq 1.\end{aligned} \tag{17}$$

That is, all eigenvalues of $L_{\mathcal{V}}^a$ are within $[0,1]$. According to (15), $L_{\mathcal{V}}^a$ and $W_{\mathcal{V}}^a$ have the same eigenvectors, and thus the kth largest eigenvalue of $W_{\mathcal{V}}^a$ is given by

$$\lambda_k(W_{\mathcal{V}}^a) = 1 - \lambda_{|\mathcal{V}|-k}(L_{\mathcal{V}}^a). \tag{18}$$

Therefore, all eigenvalues of $W_{\mathcal{V}}^a$ are bounded by $[0,1]$, which implies that $W_{\mathcal{V}}^a$ is also positive semidefinite. ∎

By comparing the second largest eigenvalue of $W_{\mathcal{M}}^c W_{\mathcal{V}}^a$ with that of $W_{\mathcal{V}}^a$, we have the following theorem with respect to the benefit of using cellular communication links.

Theorem 2. *Given $\mathcal{M}\subseteq\mathcal{V}$, $M\geq 2$, and the weight matrices $W_{\mathcal{V}}^a$ and $W_{\mathcal{M}}^c$, we have $\lambda_2(W_{\mathcal{M}}^c W_{\mathcal{V}}^a) \leq \lambda_2(W_{\mathcal{V}}^a)$.*

Proof: Since both $W_{\mathcal{M}}^c$ and $W_{\mathcal{V}}^a$ are symmetric and positive semidefinite, we have $\sum_{i=1}^k \lambda_i(W_{\mathcal{M}}^c W_{\mathcal{V}}^a) \leq \sum_{i=1}^k \lambda_i(W_{\mathcal{V}}^a)\lambda_i(W_{\mathcal{M}}^c)$ for any $k \in \{1,2,\cdots,|\mathcal{V}|\}$ [30]. Letting $k=2$, we have

$$\lambda_2(W_{\mathcal{M}}^c W_{\mathcal{V}}^a) \leq \sum_{i=1,2}\lambda_i(W_{\mathcal{V}}^a)\lambda_i(W_{\mathcal{M}}^c) - \lambda_1(W_{\mathcal{M}}^c W_{\mathcal{V}}^a). \tag{19}$$

According to the Perron-Frobenius theory [31], since the graph associated with matrix $W_{\mathcal{V}}^a$ is strongly connected, the Markov chain associated with $W_{\mathcal{V}}^a$ is irreducible. Based on Lemma 3, the multiplicity is 1 for eigenvalue 1 with respect to $W_{\mathcal{V}}^a$, i.e., $\lambda_1(W_{\mathcal{V}}^a)=1$ and $\lambda_k(W_{\mathcal{V}}^a)<1$ for $1<k\leq|\mathcal{V}|$. Suppose $W_{\mathcal{M}}^c W_{\mathcal{V}}^a = [\omega_{\mathcal{M}\mathcal{V}}^{ca}(i,j)]_{|\mathcal{V}|\times|\mathcal{V}|}$, and consider an arbitrary element $\omega_{\mathcal{M}\mathcal{V}}^{ca}(i,j)$ such that the corresponding element in $W_{\mathcal{V}}^a$ satisfies $\omega_{\mathcal{V}}^a(i,j)>0$. Then, we have

$$\omega_{AR}^{ac}(i,j) = \sum_{m\in\mathcal{V}}\omega_{\mathcal{M}}^c(i,m)\omega_{\mathcal{V}}^a(m,j) \geq \omega_{\mathcal{M}}^c(i,i)\omega_{\mathcal{V}}^a(i,j) > 0 \tag{20}$$

where the first inequality holds since all elements in $W_{\mathcal{M}}^c$ and $W_{\mathcal{V}}^a$ are non-negative, and the second inequality holds since $\omega_{\mathcal{M}}^c(i,i)>0$ for all $i\in\mathcal{V}$ according to (12). Therefore, we can conclude that the Markov chain associated with $W_{\mathcal{M}}^c W_{\mathcal{V}}^a$ is irreducible, given that the Markov chain associated with $W_{\mathcal{V}}^a$ is irreducible. Based on Lemma 3, we have $\lambda_1(W_{\mathcal{M}}^c W_{\mathcal{V}}^a)=1$ while $\lambda_k(W_{\mathcal{M}}^c W_{\mathcal{V}}^a)<1$ for $1<k\leq|\mathcal{V}|$. Taking into account (19), we have

$$\begin{aligned}\lambda_2(W_{\mathcal{M}}^c W_{\mathcal{V}}^a) &\leq \lambda_2(W_{\mathcal{V}}^a)\lambda_2(W_{\mathcal{M}}^c) + \lambda_1(W_{\mathcal{V}}^a)\lambda_1(W_{\mathcal{M}}^c)\\ &\quad - \lambda_1(W_{\mathcal{M}}^c W_{\mathcal{V}}^a)\\ &= \lambda_2(W_{\mathcal{V}}^a)\lambda_2(W_{\mathcal{M}}^c) + 1 - 1\\ &= \lambda_2(W_{\mathcal{V}}^a)\lambda_2(W_{\mathcal{M}}^c)\end{aligned} \tag{21}$$

where the first equality holds since the largest eigenvalues of $W_{\mathcal{V}}^a$, $W_{\mathcal{M}}^c$, and $W_{\mathcal{M}}^c W_{\mathcal{V}}^a$ are equal to 1. On the other hand, since all eigenvalues of $W_{\mathcal{M}}^c$ are less than or equal to 1, we have $\lambda_2(W_{\mathcal{M}}^c W_{\mathcal{V}}^a) \leq \lambda_2(W_{\mathcal{V}}^a)$ based on (21). ∎

Theorem 2 indicates that the convergence speed of multiagent coordination can be improved by using the cellular

[5]Obviously, the doubly stochastic matrices $W_{\mathcal{V}}^a$, $W_{\mathcal{M}}^c$, and $W_{\mathcal{M}}^c W_{\mathcal{V}}^a$ can be considered as the transition matrices of Markov chains with a common state space $\mathcal{V}$.

communication links. On the other hand, since both $W^c_{\mathcal{M}}$ and $W^a_{\mathcal{V}}$ are symmetric and positive semidefinite, the lower bound of $\sum_{i=1}^{k} \lambda_i(W^c_{\mathcal{M}} W^a_{\mathcal{V}})$ for any $k \in \{1, 2, \cdots, |\mathcal{V}|\}$ is given by

$$\sum_{i=1}^{k} \lambda_i(W^c_{\mathcal{M}} W^a_{\mathcal{V}}) \geq \max_{m_1,\cdots,m_k} \sum_{i=1}^{k} \lambda_{|\mathcal{V}|-m_i+1}(W^a_{\mathcal{V}})\lambda_{m_i}(W^c_{\mathcal{M}}) \tag{22}$$

where $1 \leq m_1 < m_2 < \cdots < m_k \leq |\mathcal{V}|$ are ordered integers [30]. Denote the lower and upper bounds of $\lambda_2(W^c_{\mathcal{M}} W^a_{\mathcal{V}})$ with respect to $\mathcal{M}$ as $\theta(\mathcal{M})$ and $\varphi(\mathcal{M})$, respectively. Letting $k = 2$ in (22) and taking into account (21), we have

$$\begin{aligned} \theta(\mathcal{M}) = \max_{1 \leq m_1 < m_2 \leq |\mathcal{V}|} \{&\lambda_{|\mathcal{V}|-m_1+1}(W^a_{\mathcal{V}})\lambda_{m_1}(W^c_{\mathcal{M}}) \\ &+ \lambda_{|\mathcal{V}|-m_2+1}(W^a_{\mathcal{V}})\lambda_{m_2}(W^c_{\mathcal{M}})\} - 1 \end{aligned} \tag{23}$$

$$\varphi(\mathcal{M}) = \lambda_2(W^a_{\mathcal{V}})\lambda_2(W^c_{\mathcal{M}}). \tag{24}$$

Based on $\mathcal{M}$, we consider another set $\mathcal{M}'$ with more activated cellular communication devices such that $\mathcal{M}' \subseteq \mathcal{B}$ and $\mathcal{M} \subseteq \mathcal{M}'$. Obviously, we have $M \leq |\mathcal{M}'|$. For the potential benefit of activating more cellular communication devices, we have the following proposition.

Proposition 1. *Given $M \geq 2$ and $\mathcal{M} \subseteq \mathcal{M}'$, we have $\theta(\mathcal{M}') \leq \theta(\mathcal{M})$ and $\varphi(\mathcal{M}') \leq \varphi(\mathcal{M})$.*

Proof: According to the proof of Lemma 4, the eigenvalues of $W^c_{\mathcal{M}'}$ include $|\mathcal{M}'| - 1$ zeros and $|\mathcal{V}| - |\mathcal{M}'| + 1$ ones. Therefore, we have $\lambda_k(W^c_{\mathcal{M}'}) \leq \lambda_k(W^c_{\mathcal{M}})$ for any $1 \leq k \leq |\mathcal{V}|$. Substituting this result in (23) and (24), we can easily verify $\theta(\mathcal{M}') \leq \theta(\mathcal{M})$ and $\varphi(\mathcal{M}') \leq \varphi(\mathcal{M})$. ■

V. Hierarchical Multiagent Coordination

Hierarchical multiagent coordination utilizes the network topology information for wireless link scheduling and clustering. Each of the dual-mode nodes in $\mathcal{M}$ is considered as a cluster head. As shown in Fig. 2(c), the hierarchical multiagent coordination consists of two levels. The first and second levels are performed via the ad hoc network and cellular network, respectively. Then, the dual-mode nodes in $\mathcal{M}$ broadcast (BC) the results based on the second level of multiagent coordination to the nodes within each cluster via the ad hoc network. Since network topology information is available, the wireless links can be scheduled efficiently. Moreover, given the value of M, the selection of nodes in $\mathcal{M}$ and the node clustering can be optimized. Frequency reuse is considered such that the communication links within different clusters are interference free.

A. Deterministic Ad Hoc Communication Link Scheduling

Compared with the random access, deterministic scheduling improves the efficiency of information exchange by increasing the number of concurrent transmissions [11]. Denote the node set in the cluster corresponding to node m ($m \in \mathcal{M}$) as $\mathcal{Q}_m$. For each iteration, each node in $\mathcal{Q}_m$ broadcasts its own state values once. Suppose each broadcast corresponds to one time slot with duration T_B. Denote the deterministic scheduling scheme for the nodes in $\mathcal{Q}_m$ as $\mathfrak{D}_{\mathcal{Q}_m} = \{\mathcal{D}^s_{\mathcal{Q}_m} | s \in \{1, 2, \cdots, S_{\mathcal{Q}_m}\}\}$, where $\mathcal{D}^s_{\mathcal{Q}_m}$ represents the set of nodes scheduled to broadcast during time slot s, and $S_{\mathcal{Q}_m}$ is the number of time slots required to complete an iteration. The objective of the deterministic scheduling is to construct a broadcast sequence $\mathfrak{D}_{\mathcal{Q}_m}$ which uses the minimum number of time slots to complete the broadcasts of all nodes in $\mathcal{Q}_m$, given by

Algorithm 1 Deterministic Scheduling Algorithm

Input: $\mathcal{Q}_m$, $\mathcal{N}_i$ ($i \in \mathcal{Q}_m$);
Output: $\mathfrak{D}_{\mathcal{Q}_m}$, $S_{\mathcal{Q}_m}$;
1: Initialize: $S = 1$, $\mathcal{Q}'_m = \mathcal{Q}_m$, and $\mathcal{D}^1_{\mathcal{Q}_m} = \emptyset$;
2: **while** $\cup_{s \in \{1,2,\cdots,S\}} \mathcal{D}^s_{\mathcal{Q}_m} \neq \mathcal{Q}_m$ **do**
3: Calculate the maximum independent set of $\mathcal{G}_{\mathcal{Q}'_m}$ and denote the vertex set as $\mathcal{D}^S_h$;
4: $\mathcal{Q}'_m = \mathcal{Q}_m - \cup_{s \in \{1,2,\cdots,S\}} \mathcal{D}^s_{\mathcal{Q}_m}$;
5: Update $S \leftarrow S + 1$;
6: **end while**
7: **return** $\mathfrak{D}_{\mathcal{Q}_m} = \{\mathcal{D}^s_{\mathcal{Q}_m} | s \in \{1, 2, \cdots, S_{\mathcal{Q}_m}\}\}$, $S_{\mathcal{Q}_m} = S$

$$(\mathbf{P2}) \quad \min_{\mathfrak{D}_{\mathcal{Q}_m}} \quad S_{\mathcal{Q}_m} \tag{25}$$

$$\text{subject to} \quad (\mathcal{N}_{v_1} \cup \{v_1\}) \cap (\mathcal{N}_{v_2} \cup \{v_2\}) = \emptyset, \quad v_1, v_2 \in \mathcal{D}^s_{\mathcal{Q}_m}, \ s \in \{1, 2, \cdots, S_{\mathcal{Q}_m}\} \tag{26}$$

$$\cup_{s \in \{1,2,\cdots,S_{\mathcal{Q}_m}\}} \mathcal{D}^s_{\mathcal{Q}_m} = \mathcal{Q}_m \tag{27}$$

$$\sum_{s \in \{1,2,\cdots,S_{\mathcal{Q}_m}\}} \sum_{n \in \mathcal{Q}_m} I_{n \in \mathcal{D}^s_{\mathcal{Q}_m}} = 1. \tag{28}$$

Constraint (26) indicates that there is no collision for the concurrent broadcasts during each time slot, while constraints (27) and (28) guarantee that each node broadcasts exactly once for each iteration. Problem P2 defines an integer programming problem which cannot be solved efficiently [32] [33]. In order to reduce the computational complexity, we consider a greedy algorithm, Algorithm 1. For each time slot, the algorithm maximizes the number of concurrent (collision-free) broadcasts. Note that in step 1, $\mathcal{Q}'_m$ represents the set of nodes which have not completed the broadcast. In step 3, $\mathcal{G}_{\mathcal{Q}'_m}$ denotes a directed graph corresponding to the nodes in $\mathcal{Q}'_m$ based on the ad hoc network, i.e., there is an edge from node i to node j ($i, j \in \mathcal{Q}'_m$) if and only if $j \in \mathcal{N}_i$, and vice versa. The maximum independent set can be calculated based on existing methods or heuristic algorithms [34].

B. Iteration via Cellular Network

Similar to the single-stage multiagent coordination scheme, all nodes in $\mathcal{M}$ are involved in the iteration via the cellular network. Denote the weight matrix with respect to the iteration via the cellular network as $W^h_{\mathcal{M}}(v, n) = [\omega^h_{\mathcal{M}}(v, n)]_{M \times M}$. Since each node $m \in \mathcal{M}$ is the cluster head of a set $\mathcal{Q}_m$ of nodes, the weight values should account for the cluster size, given by $\omega^h_{\mathcal{M}}(v, n) = |\mathcal{Q}_n|/|\mathcal{V}|$ for all $v, n \in \mathcal{M}$. Consider the information discovery of the average value of the aggregated capacity of type g DG units. Given a sufficiently large duration for the iterations via the ad hoc network (T_A), we have

$$\lim_{T_A \to \infty} \bar{X}_g(i, T_A) = \frac{1}{|\mathcal{Q}_m|} \sum_{v \in \mathcal{Q}_m} x_{gv}, \ i \in \mathcal{Q}_m. \tag{29}$$

Algorithm 2 Clustering Algorithm

Input: $\mathcal{V}$, $\mathcal{B}$, $\mathcal{N}_v$ $(v \in \mathcal{V})$, M;
Output: $\mathcal{M}$, $\mathcal{Q}_m$, $m \in \mathcal{M}$;
1: Initialize: $\mathcal{M} = \{m\}$ for any $m \in \mathcal{B}$, $Q_m = \mathcal{V}$;
2: **for** $i = 2$ to M **do**
3: $\quad m' = \arg\max_{m \in \mathcal{M}} \{|\mathcal{Q}_m| \mid |\mathcal{Q}_m \cap \mathcal{B}| \geq 2\}$;
4: $\quad \mathcal{V}' = \mathcal{Q}_{m'}$, $\mathcal{B}' = \mathcal{Q}_{m'} \cap \mathcal{B}$;
5: $\quad$ Update $\mathcal{M} \leftarrow (\mathcal{M} \setminus m') \cup f(\mathcal{V}', \mathcal{B}')$;
6: $\quad$ Update $\mathcal{Q}_m$ for $m \in f(\mathcal{V}', \mathcal{B}')$;
7: **end for**
8: **return** $\mathcal{M}$, $\mathcal{Q}_m$, $m \in \mathcal{M}$

After the iteration via the cellular network, the state value broadcasted by each node in $\mathcal{M}$ to the cluster members is given by

$$\begin{aligned}&\sum_{m \in \mathcal{M}} \frac{|\mathcal{Q}_m|}{|\mathcal{V}|} \cdot \frac{1}{|\mathcal{Q}_m|} \sum_{v \in \mathcal{Q}_m} x_{gv} \\ &= \frac{1}{|\mathcal{V}|} \sum_{m \in \mathcal{M}} \sum_{v \in \mathcal{Q}_m} x_{gv} = \frac{1}{|\mathcal{V}|} \sum_{v \in \mathcal{V}} x_{gv} = \bar{X}_g. \qquad (30)\end{aligned}$$

Therefore, the convergence of the hierarchical multiagent coordination is guaranteed.

C. Performance Analysis and Node Clustering

Since the cluster sizes ($|\mathcal{Q}_m|$) corresponding to the nodes $m \in \mathcal{M}$ are different, the performance of the hierarchical multiagent coordination is related to the clustering algorithm. The error of the hierarchical multiagent coordination at time T is given by

$$\begin{aligned}&||\Phi_{g,\mathcal{V}}(T)||_2 \\ &= \sqrt{|\mathcal{V}| \left[\left(\sum_{m \in \mathcal{M}} \frac{|\mathcal{Q}_m|}{|\mathcal{V}|} \bar{X}_g(m, T_A) \right) - \bar{X}_g \right]^2} \\ &= \sqrt{\frac{1}{|\mathcal{V}|} \left[\sum_{m \in \mathcal{M}} |\mathcal{Q}_m| \left(\bar{X}_g(m, T_A) - \bar{X}_g \right) \right]^2} \\ &\leq \sqrt{\sum_{m \in \mathcal{M}} |\mathcal{Q}_m| \left(\bar{X}_g(m, T_A) - \bar{X}_g \right)^2} \\ &\leq \sqrt{\sum_{m \in \mathcal{M}} |\mathcal{Q}_m| \cdot ||\Phi_{g,\mathcal{Q}_m}(T_A)||_2^2} \\ &\leq \sqrt{\sum_{m \in \mathcal{M}} |\mathcal{Q}_m| [\lambda_2(W^a_{\mathcal{Q}_m})]^{\lfloor \frac{2T_A}{S_{\mathcal{Q}_m} T_B} \rfloor} ||\Phi_{g,\mathcal{Q}_m}(0)||_2^2} \\ &\leq ||\Phi_{g,\mathcal{V}}(0)||_\infty \sqrt{\sum_{m \in \mathcal{M}} |\mathcal{Q}_m|^2 [\lambda_2(W^a_{\mathcal{Q}_m})]^{\lfloor \frac{2T_A}{S_{\mathcal{Q}_m} T_B} \rfloor}} \qquad (31)\end{aligned}$$

where the second equality holds since $\sum_{m \in \mathcal{M}} |\mathcal{Q}_m| = |\mathcal{V}|$, and $||\Phi_{g,\mathcal{V}}(0)||_\infty$ equals the largest element of the initial disagreement vector. Compared with the multiagent coordination via the ad hoc network, the benefit of the hierarchical multiagent coordination scheme is based on the potentially smaller $S_{\mathcal{Q}_m}$ and $\lambda_2(W^a_{\mathcal{Q}_m})$ for smaller graphs, i.e., $\mathcal{Q}_m \subset \mathcal{V}$. Similar observation can be obtained by decomposing an ad hoc network with long-range links [35].

According to (31), for a given number of activated cellular communication devices M, the convergence speed of the hierarchical multiagent coordination is determined by $\sum_{m \in \mathcal{M}} |\mathcal{Q}_m|^2 [\lambda_2(W^a_{\mathcal{Q}_m})]^{\lfloor \frac{2T_A}{S_{\mathcal{Q}_m} T_B} \rfloor}$, which needs to be minimized for all possible combinations of M nodes in $\mathcal{B}$ and all nodes in $\mathcal{V}$. However, the computational complexity is $O(|\mathcal{B}|^M |\mathcal{V}|^M)$, which is prohibitive as the network size increases. Note that the error of the hierarchical multiagent coordination scheme is dominated by the largest cluster (by a factor of $\max_{m \in \mathcal{M}} |\mathcal{Q}_m|^2$). Therefore, we consider a heuristic clustering algorithm which constructs the clusters by splitting [15] the largest cluster which includes at least two dual-mode nodes. The details are given in Algorithm 2, where the function $f(\cdot)$ is used to calculate an optimal split of a cluster with respect to a set $\mathcal{V}'$ of ad hoc nodes and a subset $\mathcal{B}'$ ($\mathcal{B}' \subseteq \mathcal{V}'$) of dual-mode nodes, given by

$$\begin{aligned}f(\mathcal{V}', \mathcal{B}') = \arg &\min_{\substack{\{m_1, m_2\} \in \mathcal{B}' \times \mathcal{B}', m_1 \neq m_2 \\ \mathcal{Q}_{m_1} \cup \mathcal{Q}_{m_2} = \mathcal{V}'}} \Bigg\{ \\ &\sum_{k=1,2} |\mathcal{Q}_{m_k}|^2 [\lambda_2(W^a_{\mathcal{Q}_{m_k}})]^{\lfloor \frac{2T_A}{S_{\mathcal{Q}_{m_k}} T_B} \rfloor} \Bigg\}. \qquad (32)\end{aligned}$$

Note that if there is only one element in a cluster $\mathcal{Q}_m$ (i.e., $|\mathcal{Q}_m| = 1$), we denote $\lambda_2(W^a_{\mathcal{Q}_m}) = 0$ since each node has accurate power generation and load information of itself. For computational simplicity, the cluster members in terms of $\mathcal{Q}_{m_1}$ and $\mathcal{Q}_{m_2}$ are determined by the shortest-distance criteria, i.e., a Voronoi diagram with two points. In a case that $\mathcal{Q}_{m'}$ cannot be split into two clusters without isolated nodes, step 3 is recalculated with respect to the second largest cluster, and so on. Since each step of the cluster splitting only takes into account all possible pairs of dual-mode nodes in one cluster, the complexity of the algorithm is $O(M|\mathcal{B}|^2)$.

VI. Communication Cost versus Energy Cost

Based on the discussions in Section IV and Section V, the error of multiagent coordination can be (potentially) reduced by activating more cellular communication devices. With more accurate information, each DG unit can make better decision on power generation for generation cost minimization. However, the communication cost increases as the number of activated cellular communication devices increases. In this section, we investigate a tradeoff between the communication and generation costs.

A. Cost Model

Consider one economic dispatch period as an example. The communication cost is a function of the number of activated cellular communication devices M. For the single-stage and hierarchical multiagent coordination schemes, the communication costs (in dollars) are, respectively, given by

$$C_C^S(M) = c_M M(M-1) E\left[T / T_I(\mathcal{V})\right] \qquad (33)$$

$$C_C^H(M) = c_M M(M-1) \qquad (34)$$

where $E\left[T / T_I(\mathcal{V})\right]$ is the average number of iterations of multiagent coordination via the ad hoc network within T. Note that the cost of single-stage multiagent coordination is enlarged by a factor of $E\left[T/T_I(\mathcal{V})\right]$ since an iteration via the cellular network is performed after each iteration via the ad hoc network.

After the multiagent coordination, denote the state values of cumulative capacity and aggregated loads obtained by node v as $\bar{\mathbf{X}}_v = \{\bar{X}_1(v,T), \bar{X}_2(v,T), \cdots, \bar{X}_G(v,T)\}$ and $\bar{Y}_v = \bar{Y}(v,T)$, respectively. Based on (4), the decentralized decision on the economic dispatch is given by $u_{gv}(\bar{\mathbf{X}}_v, \bar{Y}_v, \mathbf{c})$, where $\bar{\mathbf{X}}$ and $\bar{Y}$ are replaced by $\bar{\mathbf{X}}_v$ and $\bar{Y}_v$, respectively. Given the minimum cost $C_P^*(\mathbf{x},\mathbf{y},\mathbf{c})$ based on problem P1 which is a constant within T_D, we consider the increment in the generation cost by using inaccurate information, which is a function of M and is given by

$$\begin{aligned} C_P^I(M) = \mathrm{E}\Bigg[& c_A\Big(Y - \sum_{g\in\{1,2,\cdots,G\}} \sum_{v\in\mathcal{V}} u_{gv}(\bar{\mathbf{X}}_v, \bar{Y}_v, \mathbf{c})\Big)^+ \\ & + c_E\Big(\sum_{g\in\{1,2,\cdots,G\}} \sum_{v\in\mathcal{V}} u_{gv}(\bar{\mathbf{X}}_v, \bar{Y}_v, \mathbf{c}) - Y\Big)^+ \\ & + \sum_{g\in\{1,2,\cdots,G\}} c_g \sum_{v\in\mathcal{V}} u_{gv}(\bar{\mathbf{X}}_v, \bar{Y}_v, \mathbf{c}) \Bigg] - \mathrm{E}\left[C_P^*(\mathbf{x},\mathbf{y},\mathbf{c})\right] \end{aligned} \tag{35}$$

where the first expectation is taken with respect to the random variables $\mathbf{x}$ and $\mathbf{y}$, and the set of randomly activated cellular communication devices ($\mathcal{M}$) for the single-stage multiagent coordination scheme. Denote the incremental generation cost of the single-stage and hierarchical multiagent coordination schemes as $C_P^{IS}(M)$ and $C_P^{IH}(M)$, respectively.

B. Cost Tradeoff

The objective is to minimize the combined communication and incremental generation costs by properly selecting the number of activated cellular communication devices M. The desired value of M for the single-stage multiagent coordination is given by problem P3 as follows:

$$(\mathbf{P3}) \quad \min_{M\in\{1,2,\cdots,|\mathcal{B}|\}} \quad C_C^S(M) + C_P^{IS}(M)T_D \tag{36}$$

where the second term has a factor of T_D since we investigate the cost (in dollars) for one economic dispatch period. Similarly, we can calculate the desired value of M for the hierarchical multiagent coordination scheme. Problem P3 is an integer programming problem which is NP-hard in general. Although an exhaustive search can be used to find the solution, the computational complexity can be prohibitive because of the expectation operation in (35). Moreover, the statistics of $\mathbf{x}$ and $\mathbf{y}$ (and the network topology information with respect to the single-stage multiagent coordination scheme) may not be available for a microgrid. Therefore, an approximation of the incremental generation cost $C_P^{IS}(M)$ is indispensable for practical applications.

For a self-sustained microgrid, the power generation by the G types of DG units and loads should be balanced for most of the time. Therefore, we can approximate the incremental generation cost based on the undelivered and extra power as

$$\tilde{C}_P^{IS}(M) = (c_A - c_1)\tilde{z}_A + (c_G + c_E)\tilde{z}_E \tag{37}$$

where $\tilde{z}_A$ and $\tilde{z}_E$ are the average values of z_A and z_E observed over a certain period of time (e.g., one day) by the alternative energy sources and negative spinning reserve service providers, respectively. Note that (37) provides an upper bound of $C_P^{IS}(M)$ since the price of purchasing power from the DG units is no less than c_1 and no greater than c_G. Based on the estimate $\tilde{C}_P^{IS}(M)$, an approximation of the desired tradeoff between the communication and generation costs can be achieved without resorting to the statistics of $\mathbf{x}$ and $\mathbf{y}$, which simplifies the network optimization of microgrids. Similarly, we can use the estimate $\tilde{C}_P^{IH}(M)$ for hierarchical multiagent coordination.

VII. Numerical Results

The network topology used for simulations is shown in Fig. 3. We consider the Laurelwood neighborhood located in North-West Waterloo as a microgrid topology for the deployment of DG units and wireless devices. We plot the wind turbines, PV panels, and loads at adequate geographic locations on the map. For the generation data of wind turbines, a probability distribution of the wind speed for Waterloo is obtained from Canadian Wind Energy Atlas [36] considering the 50 kW wind turbines located at 30 m height [37]. The power curve (which is the output power as a function of instantaneous wind speed) of the actual wind turbine is used to translate wind speeds to the amount of power generations. The probability distribution follows the Weibull distribution with a shape parameter 1.94 and scale parameter 4.48 m/s. The startup, cutout, and rated wind speeds are 2 m/s, 18 m/s, and 11 m/s, respectively. For the generation data of PV panels, hourly PV performance data of Toronto (100 km away from Waterloo) is obtained from NREL (National Renewable Energy Laboratory) PVWatts™ site specific calculator [38] which determines the power production of PV panels for a given geographic location. The AC rating of the PV panels is 3.08 kW. For the demand of loads, an hourly demand is obtained from the smart meters of two residences in the Laurelwood neighborhood subscribed to Waterloo North Hydro [39]. The demand data is approximated by a normal distribution [40]. For instance, the mean and standard deviation in kWh during the on-peak hours (i.e., 9 am and 6 pm) and off-peak hours (i.e., 1 am to 7 am and 1 pm to 4 pm) are, respectively, given by (1.5, 0.43) and (0.70, 0.04). For consistency, all power generation and load data are taken during the month of June in Waterloo. The costs are 0.135, 0.802, 2.080, and 0.000 (CAD) dollar/kWh for wind turbine, PV panel [17], diesel generator, and negative spinning reserves (i.e. the cost is neglected) [4], respectively. For the heterogeneous wireless network infrastructure, the transmission range of ad hoc communication devices is 150 m with a link layer data rate 2 Mbps and a PHY header according to the IEEE 802.11 standard [41]. For the update-and-wait and update-and-continue based random access schemes, we consider each ad hoc node accesses the wireless medium with probability 0.1 [42] and a retransmission mechanism is in place to guarantee the successful broadcast. We randomly select 44 dual-mode nodes with the cellular capability as shown in Fig. 3 and consider a basic data plan of Rogers Canada with 40 dollars

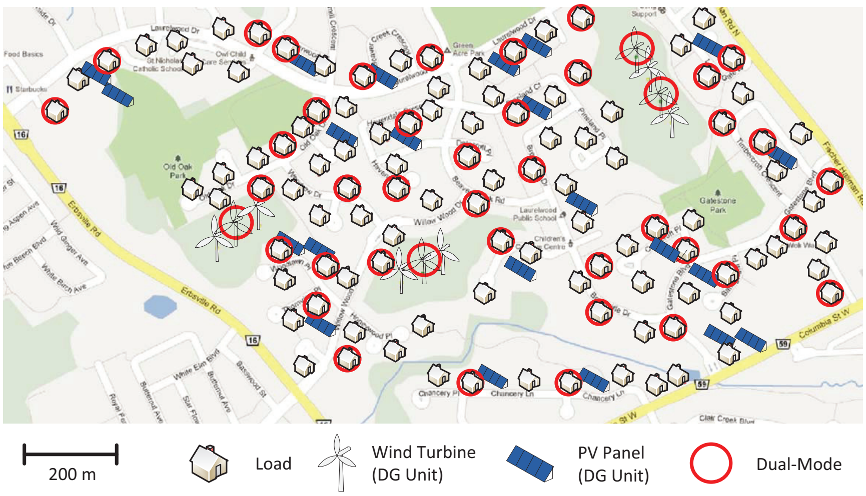

Fig. 3. The network topology for simulations.

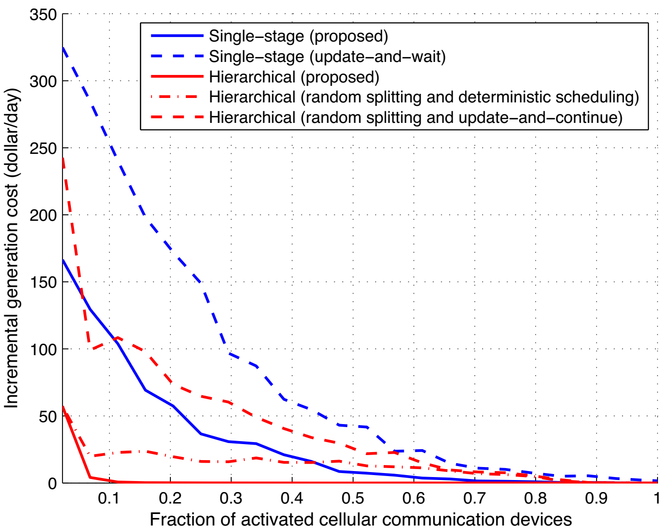

Fig. 4. Incremental generation cost (per day) versus the fraction of activated cellular communication devices.

for 100 MB data[6]. Since the power generation and demand state information can be represented by 16 bits [10], we have $c_M = 2.4 \times 10^{-6}$ dollars, which can be considered as a lower bound of communication cost since packetization overhead is not included. The durations of the economic dispatch and information exchange periods are $T_D = 300$ s (i.e., $\frac{1}{12}$ h) and $T(= T_A) = 2$ s, respectively [2] [3]. The capacity of DG units and the loads are randomly generated for each economic dispatch period during the simulations. For a fair comparison, we focus on the average costs since random selection of dual-mode nodes is used by our proposed single-stage multiagent coordination scheme and random cluster splitting is studied in the following performance evaluation. Each simulation run lasts for one day from which the communication and generation costs are calculated, and the results are averaged over 30 days.

[6]It is worth mentioning that this is a service plan for cell phone users. How to customize the plan for microgrid operation is still an open issue and left for our future work.

Fig. 4 shows the incremental generation cost ($C_P^I(M)$) on a daily basis versus the fraction of activated cellular communication devices ($M/|\mathcal{B}|$). As we can see, the generation costs of both schemes decrease as the fraction of activated cellular communication devices increases since more cellular communication links can (potentially) improve the network connectivity and thus reduce the error in multiagent coordination. The update-and-continue based random access scheme which is used by our proposed single-stage multiagent coordination scheme can reduce the generation cost as compared with the update-and-wait scheme by reducing the duration of each iteration via the ad hoc network. The proposed hierarchical multiagent coordination scheme achieves the lowest generation cost based on deterministic scheduling and efficient clustering. For comparison, if random cluster splitting (without information of the cluster size and eigenvalues of weight matrices) is used, the generation cost decreases slowly with the fraction of activated cellular communication devices. Moreover, if update-and-continue based random access is also used (without network topology information for wireless link scheduling), the generation cost further increases because of an increased iteration duration within each cluster. The generation cost is even higher than the single-stage counterpart since the error of the hierarchical multiagent coordination scheme is dominated by the potential large clusters as a result of random cluster splitting, according to our analysis in Subsection V-C.

Taking account of the cost of using cellular communication links, a tradeoff between the communication and incremental generation costs is shown in Fig. 5. For presentation clarity, we normalize the combined communication and generation costs of both schemes by their maximum actual costs, given by 166.5 and 57.2 dollars, respectively. We can see that, the communication and generation costs are comparable with each other. As the fraction of activated cellular communication devices increases, the normalized cost first decreases since the generation cost decreases. Then, the normalized cost increases as the communication cost increases and exceeds the decrement in the generation cost. Therefore, there is a desired tradeoff point between the communication and generation costs for both single-stage and hierarchical multiagent coordi-

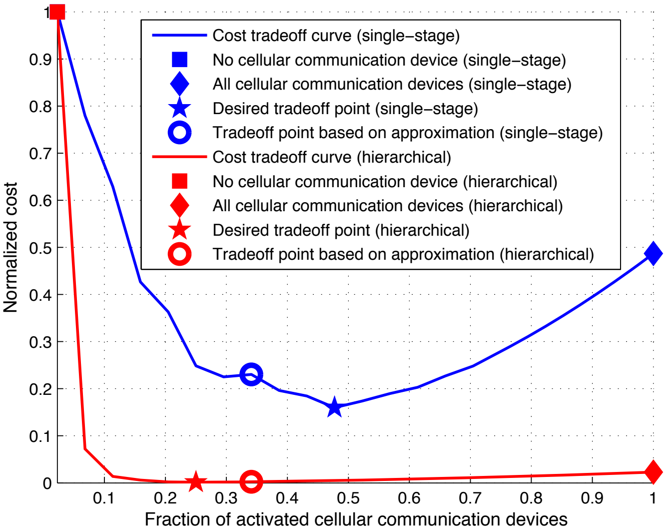

Fig. 5. Tradeoff between the communication and generation costs.

nation schemes, which provides the minimum normalized cost. Since the network topology information is used by the hierarchical multiagent coordination scheme, the desired tradeoff is achieved by activating less cellular communication devices. The normalized cost achieved at the tradeoff point based on the approximation of incremental generation cost is close to that of the desired tradeoff point, which implies a good estimate for the desired value of M. The normalized cost based on the existing schemes without using cellular communication devices [10] or with all cellular communication devices (or equivalently, all long-range links [35]) being activated is also shown. We can see that, the existing schemes can only achieve the boundary points of the cost tradeoff curves and may not be efficient in minimizing the combined communication and generation costs.

VIII. Conclusions and Future Work

In this paper, we have introduced a decentralized economic dispatch approach for microgrids such that each DG unit makes local decisions on power generation based on a multiagent coordination with guaranteed convergence. A heterogeneous wireless network architecture has been established accordingly. Each node uses an ad hoc communication device for basic information exchange, while some dual-mode nodes are equipped with optional cellular communication devices which can be activated to improve the convergence speed of multiagent coordination. Two multiagent coordination schemes have been proposed to utilize the cellular communication links based on the single-stage and hierarchical operation modes, respectively. Numerical results indicate that our propose schemes can better utilized the cellular communication links and achieve better tradeoff between the communication and generation costs in comparison with the existing schemes.

Future work includes the decentralized clock synchronization in microgrids for real-time monitoring and control [43] and the broadcast gossip which does not require two-way information exchange [44]. Moreover, an optimization of the decentralized economic dispatch approach by taking account of the prediction error of power generation and load information [16] and the security issues in wireless networks [45] [46] is an interesting topic and needs further investigation.

Acknowledgment

The authors wish to thank A. S. A. Awad from Energy and Power Systems Group at the University of Waterloo for his helpful discussions.

Appendix: Proof of Theorem 1

Denote the economic dispatch policy given by (4) as $\mathbf{u}^* = \{u^*_{gv} | g \in \{1,2,\cdots,G\}, v \in \mathcal{V}\}$. We consider two cases with respect to the relation between the cumulative capacity and aggregated loads: Case 1): The aggregated loads cannot be satisfied based on the power generation of DG units, i.e., $\sum_{g\in\{1,2,\cdots,G\}} \bar{X}_g < \bar{Y}$ (or equivalently, $\sum_{g\in\{1,2,\cdots,G\}} X_g < Y$); Case 2): The aggregated loads can be satisfied based on the power generation of DG units, i.e., $\sum_{g\in\{1,2,\cdots,G\}} \bar{X}_g \ge \bar{Y}$ (or equivalently, $\sum_{g\in\{1,2,\cdots,G\}} X_g \ge Y$). The proofs of both cases are completed by contradiction.

Case 1): According to the first case of policy (4), all DG units should operate at the maximum capacity, i.e., $u^*_{gv} = x_{gv}$. Suppose another policy $\mathbf{u}' \ne \mathbf{u}^*$ is optimal. Then, there exists at least one pair (i,j) such that $u'_{ij} < x_{ij}$. Consider another policy $\mathbf{u}'' = \{u''_{ij}, u'_{gv} | g \in \{1,2,\cdots,G\}, v \in \mathcal{V}, (g,v) \ne (i,j)\}$ with $u''_{ij} \in (u'_{ij}, x_{ij}]$. Then, the generation cost based on policy $\mathbf{u}''$ is given by

$$\begin{aligned} C_P(\mathbf{x},\mathbf{y},\mathbf{c},\mathbf{u}'') &= c_A(Y - \sum_{g\in\{1,2,\cdots,G\}} \sum_{\substack{v\in\mathcal{V}\\(g,v)\ne(i,j)}} u'_{gv} - u''_{ij}) \\ &\quad + \sum_{g\in\{1,2,\cdots,G\}} \sum_{\substack{v\in\mathcal{V}\\(g,v)\ne(i,j)}} c_g u'_{gv} + c_i u''_{ij} \\ &= C_P(\mathbf{x},\mathbf{y},\mathbf{c},\mathbf{u}') + (c_i - c_A)(u''_{ij} - u'_{ij}). \end{aligned} \tag{38}$$

Since $c_i < c_A$ and $u''_{ij} > u'_{ij}$, we have $C_P(\mathbf{x},\mathbf{y},\mathbf{c},\mathbf{u}'') < C_P(\mathbf{x},\mathbf{y},\mathbf{c},\mathbf{u}')$, which contradicts with the assumption that $\mathbf{u}'$ is optimal.

Case 2): Based on Lemma 2, the aggregated power generation of the DG units and the aggregated loads should be balanced. In other words, a policy different from $\mathbf{u}^*$ should have at least two different elements with respect to the decisions on power generation. Because of space limitation, we consider a policy $\mathbf{u}'$ with exactly two different elements from $\mathbf{u}^*$, i.e., $\mathbf{u}' = \{u'_{ij}, u'_{mn}, u^*_{gv} | g \in \{1,2,\cdots,G\}, v \in \mathcal{V}, (g,v) \notin \{(i,j),(m,n)\}\}$ with $u'_{ij} \ne u^*_{ij}$ and $u'_{mn} \ne u^*_{mn}$. An extension of the proof for a policy with more different elements is straightforward. Note that the two elements correspond to two different types of DG units with different generation costs. Otherwise, the total generation cost is the same based on the power balance equation. Suppose $1 \le i < m \le G$ and the policy $\mathbf{u}'$ is optimal. Since $\sum_{g\in\{1,2,\cdots,G\}} X_g \ge Y$, we can define $g^* = \arg\max_{g\in\{1,2,\cdots,G\}} \left\{\sum_{i\in\{1,2,\cdots,g\}} X_i \le Y\right\}$. Then, we calculate the generation costs with respect to two different relations between i and g^*, i.e., $i \le g^*$ and $i > g^*$, respectively. If $i \le g^*$, we have $u'_{ij} < u^*_{ij}$ since $u^*_{ij} = x_{ij}$ according to (4). Moreover, we have $m > g^*$ and $u'_{mn} =$

$u_{ij}^* + u_{mn}^* - u_{ij}'$ to balance the power generation and loads. Then, the generation cost based on the economic dispatch policy $\mathbf{u}'$ is given by

$$\begin{aligned} C_P(\mathbf{x},\mathbf{y},\mathbf{c},\mathbf{u}') = & \sum_{g\in\{1,2,\cdots,G\}} c_g \sum_{v\in\mathcal{V}} u_{gv}^* I_{(g,v)\notin\{(i,j),(m,n)\}} \\ & + c_i u_{ij}' + c_m(u_{ij}^* + u_{mn}^* - u_{ij}') \\ & = C_P(\mathbf{x},\mathbf{y},\mathbf{c},\mathbf{u}^*) + (c_i - c_m)(u_{ij}' - u_{ij}^*) \\ & > C_P(\mathbf{x},\mathbf{y},\mathbf{c},\mathbf{u}^*) \end{aligned} \tag{39}$$

where I_A is an indication function which equals 1 if A is true and 0 otherwise, while the inequality holds since $c_i < c_m$ and $u_{ij}' < u_{ij}^*$. The result in (39) contradicts with the assumption that $\mathbf{u}'$ is optimal. On the other hand, if $i > g^*$, we have $m > i > g^*$ and the proof follows similar steps. For other combinations of i and m, the generation and loads cannot be balanced. This completes the proof.

REFERENCES

[1] S. Chowdhury, S. P. Chowdhury, and P. Crossley, *Microgrids and Active Distribution Networks*. Institution of Engineering and Technology, 2009.

[2] Y. V. Makarov, C. Loutan, J. Ma, and P. de Mello, "Operational impacts of wind generation on California power systems," *IEEE Trans. Power Syst.*, vol. 24, no. 2, pp. 1039–1050, May 2009.

[3] V. Vittal, "The impact of renewable resources on the performance and reliability of the electricity grid," *Bridge on Electricity Grid*, vol. 40, no. 1, Spring 2010.

[4] H. Moraisa, P. Kadarb, P. Fariaa, Z. A. Valea, and H. M. Khodra, "Optimal scheduling of a renewable micro-grid in an isolated load area using mixed-integer linear programming," *Renewable Energy*, vol. 35, no. 1, pp. 151–156, Jan. 2010.

[5] J. Hetzer, D. C. Yu, and K. Bhattarai, "An economic dispatch model incorporating wind power," *IEEE Trans. Energ. Conver.*, vol. 23, no. 2, pp. 603–611, Jun. 2008.

[6] E. M. Constantinescu, V. M. Zavala, M. Rocklin, S. Lee, and M. Anitescu, "A computational framework for uncertainty quantification and stochastic optimization in unit commitment with wind power generation," *IEEE Trans. Power Syst.*, vol. 26, no. 1, pp. 431–441, Feb. 2011.

[7] F. Katiraei, R. Iravani, N. Hatziargyriou, and A. Dimeas, "Microgrids management," *IEEE Power and Energ. Mag.*, vol. 6, no. 3, pp. 54–65, May-Jun. 2008.

[8] H. Farhangi, "The path of the smart grid," *IEEE Power and Energ. Mag.*, vol. 8, no. 1, pp. 18–28, Jan.-Feb. 2010.

[9] W. Gatterbauer. *Interdependencies of Electricity Market Characteristics and Bidding Strategies of Power Producers*. Master thesis, Massachusetts Institute of Technology, Cambridge, 2002.

[10] Y. Xu and W. Liu, "Novel multiagent based load restoration algorithm for microgrids," *IEEE Trans. Smart Grid*, vol. 2, no. 1, pp. 152–161, Mar. 2011.

[11] H. Liang, A. Abdrabou, B. J. Choi, W. Zhuang, X. Shen, and A. S. A. Awad, "Multiagent coordination in microgrids via wireless networks," *IEEE Wireless Commun.*, under review.

[12] A. Tahbaz-Salehi and A. Jadbabaie, "Small world phenomenon, rapidly mixing Markov chains, and average consensus algorithms," in *Proc. IEEE CDC'07*, pp. 276–281, Dec. 2007.

[13] S. Vanka, M. Haenggi, and V. Gupta, "Convergence speed of the consensus algorithm with interference and sparse long-range connectivity," *IEEE J. Sel. Topics Signal Process.*, vol. 5, no. 4, pp. 855–865, Aug. 2011.

[14] H. Li and W. Zhang, "QoS routing in smart grid," in *Proc. IEEE GLOBECOM'10*, Dec. 2010.

[15] D. Niyato, L. Xiao, and P. Wang, "Machine-to-machine communications for home energy management system in smart grid," *IEEE Commun. Mag.*, vol. 49, no. 4, pp. 53–59, Apr. 2011.

[16] A. Kusiak, H. Zheng, and Z. Song, "Short-term prediction of wind farm power: a data mining approach," *IEEE Trans. Energ. Convers.*, vol. 24, no. 1, pp. 125–136, Mar. 2009.

[17] Ontario power authority. http://fit.powerauthority.on.ca/.

[18] H. Liang, B. J. Choi, W. Zhuang, and X. Shen, "Towards optimal energy store-carry-and-deliver for PHEVs via V2G system," in *Proc. IEEE INFOCOM'12*, Mar. 2012.

[19] V. V. Viswanathan and M. Kintner-Meyer, "Second use of transportation batteries: maximizing the value of batteries for transportation and grid services," *IEEE Trans. Veh. Technol.*, vol. 60, no. 7, pp. 2963–2970, Sept. 2011.

[20] T. K. Lee, B. Adornato, and Z. S. Filipi, "Synthesis of real-world driving cycles and their use for estimating PHEV energy consumption and charging opportunities: case study for Midwest/U.S.," *IEEE Trans. Veh. Technol.*, vol. 60, no. 9, pp. 4153–4163, Nov. 2011.

[21] S. Galli, A. Scaglione, and Z. Wang, "For the grid and through the grid: the role of power line communications in the smart grid," *Proc. IEEE*, vol. 99, no. 6, pp. 998–1027, Jun. 2011.

[22] 3GPP. http://www.3gpp.org/.

[23] W. Song and W. Zhuang, "Multi-service load sharing for resource management in the cellular/WLAN integrated network," *IEEE Trans. Wireless Commun.*, vol. 8, no. 2, pp. 725–735, Feb. 2009.

[24] M. Ismail and W. Zhuang, "A distributed multi-service resource allocation algorithm in heterogeneous wireless access medium," *IEEE J. Sel. Areas Commun.*, vol. 30, no. 2, pp. 425-432, Feb. 2012.

[25] W. Song, Y. Cheng, and W. Zhuang, "Improving voice and data services in cellular/WLAN integrated network by admission control," *IEEE Trans. Wireless Commun.*, vol. 6, no. 11, pp. 4025-4037, Nov. 2007.

[26] V. Blondel, J. Hendrickx, A. Olshevsky, and J. Tsitsiklis, "Convergence in multiagent coordination, consensus, and flocking," *Proc. IEEE CDC-ECC*, pp. 2996–3000, Dec. 2005.

[27] R. Olfati-Saber, J. Fax, and R. Murray, "Consensus and cooperation in networked multi-node systems," *Proc. IEEE*, vol. 95, pp. 215–233, Jan. 2007.

[28] L. Xiao and S. Boyd, "Fast linear iterations for distributed averaging," in *Proc. IEEE CDC'03*, vol. 5, pp. 4997–5002, Dec. 2003.

[29] D. L. Isaacson and R. W. Madsen. *Markov Chains: Theory and Applications*. Wiley, New York, 1976.

[30] F. Zhang and Q. Zhang, "Eigenvalue inequalities for matrix product," *IEEE Trans. Automat. Contr.*, vol. 51, no. 9, pp. 1506–1509, Sept. 2006.

[31] C. D. Meyer. *Matrix Analysis and Applied Linear Algebra*. The Society for Industrial and Applied Mathematics (SIAM), 2000.

[32] G. L. Nemhauser and L. A. Wolsey. *Integer and Combinatorial Optimization*. New York: John Wiley & Sons, 1988.

[33] E. Liu, Q. Zhang, and K. K. Leung, "Clique-based utility maximization in wireless mesh networks," *IEEE Trans. Wireless Commun.*, vol. 10, no. 3, Mar. 2011, pp. 948–957.

[34] S. Balaji, V. Swaminathan, and K. Kannan, "A simple algorithm to optimize maximum independent set," *Advanced Modeling and Optimization*, vol. 12, no. 1, pp. 107-118, 2010.

[35] M. Epstein. *Managing Information in Networked and Multi-Agent Control Systems*. PhD thesis, California Institute of Technology, 2007.

[36] Canadian Wind Energy Atlas, http://www.windatlas.ca/.

[37] ReDriven Power Inc. 50kw Wind Turbine, http://www.redriven.ca/products/50kw-wind-turbine.

[38] NREL (National Renewable Energy Laboratory): PVWatts$^{\text{TM}}$ Site Specific Calculator, http://www.nrel.gov/rredc/pvwatts.

[39] Waterloo North Hydro. http://www.wnhydro.com/.

[40] M. He, S. Murugesan, and J. Zhang, "Multiple timescale dispatch and scheduling for stochastic reliability in smart grids with wind generation integration," in *Proc. IEEE INFOCOM'11*, Apr. 2011.

[41] Y. Xiao and J. Rosdahl, "Throughput and delay limits of IEEE 802.11," *IEEE Commun. Lett.*, vol. 6, no. 8, pp. 355–357, Aug. 2002.

[42] G. Bianchi, "Performance analysis of the IEEE 802.11 distributed coordination function," *IEEE J. Sel. Areas Commun.*, vol. 18, no. 3, pp. 535–547, Mar. 2000.

[43] B. J. Choi, H. Liang, X. Shen, and W. Zhuang, "DCS: distributed asynchronous clock synchronization in delay tolerant networks," *IEEE Trans. Parallel Distrib.*, 2012.

[44] T. C. Aysal, M. E. Yildiz, A. D. Sarwate, and A. Scaglione, "Broadcast gossip algorithms for consensus," *IEEE Trans. Singal Process.*, vol. 57, no. 7, pp. 2748–2761, Jul. 2009.

[45] M. E. Mahmoud and X. Shen, "PIS: a practical incentive system for multi-hop wireless networks," *IEEE Trans. Veh. Technol.*, vol. 59, no. 8, pp. 4012–4025, Oct. 2010.

[46] M. E. Mahmoud and X. Shen, "An integrated stimulation and punishment mechanism for thwarting packet drop in multihop wireless networks," *IEEE Trans. Veh. Technol.*, vol. 60, no. 8, pp. 3947–3962, Oct. 2011.

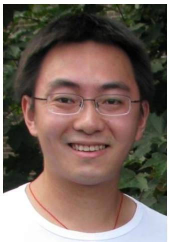

Hao Liang (S'09) received the B.Sc. degree from Nanjing University of Science and Technology, China, in 2005, and the M.Sc. degree from Southeast University, China, in 2008, both in electrical engineering. He is currently working toward a Ph.D. degree at the Department of Electrical and Computer Engineering, University of Waterloo, Canada. His current research interests are in the areas of wireless communications, wireless networking, and smart grid. He is a recipient of the Best Student Paper Award from IEEE 72nd Vehicular Technology Conference (VTC Fall-2010), Ottawa, Ontario, Canada, and a finalist for the Best Paper Award at the 31st Annual IEEE International Conference on Computer Communications (INFOCOM 2012), Orlando, Florida, USA. He served as the Technical Program Committee (TPC) Member for IEEE VTC Fall-2011 and IEEE VTC Fall-2010. He is the System Administrator of IEEE Transactions on Vehicular Technology.

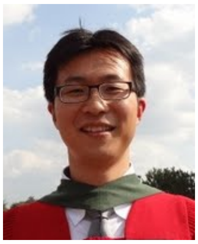

Bong Jun Choi (M'11) received the BSc (2003) and MSc (2005) degrees from Yonsei University, Seoul, Republic of Korea, both in electrical and electronics engineering, and the PhD (2011) degree from University of Waterloo, Canada, in electrical and computer engineering. He is a postdoctoral fellow at the Department of Electrical and Computer Engineering, University of Waterloo, Canada. He was a software engineer at Telecommunication Network Division of Samsung Electronics in 2005-2006. His current research focuses on energy efficiency, distributed computing, and medium access control in wireless communications and networking. He serves as an editor of KSII Transactions on Internet and Information Systems.

Atef Abdrabou (M'09) received the Ph.D. degree in 2008 from the University of Waterloo, Ontario, Canada, in electrical engineering. In 2010, he joined the Department of Electrical Engineering, UAE University, Al-Ain, Abu Dhabi, UAE, where he is an Assistant Professor. He is a co-recipient of a Best Paper Award of IEEE WCNC 2010.

Dr. Abdrabou has been awarded the National Science and Engineering Research Council (NSERC) of Canada postdoctoral fellowship in 2009. His current research interests include network resource management, QoS provisioning and information dissemination in self-organizing wireless networks.

Weihua Zhuang (M93-SM01-F'08) has been with the Department of Electrical and Computer Engineering, University of Waterloo, Canada, since 1993, where she is a Professor and a Tier I Canada Research Chair in Wireless Communication Networks. Her current research focuses on resource allocation and QoS provisioning in wireless networks. She is a co-recipient of the Best Paper Awards from the IEEE Multimedia Communications Technical Committee in 2011, IEEE Vehicular Technology Conference (VTC) Fall 2010, IEEE Wireless Communications and Networking Conference (WCNC) 2007 and 2010, IEEE International Conference on Communications (ICC) 2007, and the International Conference on Heterogeneous Networking for Quality, Reliability, Security and Robustness (QShine) 2007 and 2008. She received the Outstanding Performance Award 4 times since 2005 from the University of Waterloo, and the Premier's Research Excellence Award in 2001 from the Ontario Government. Dr. Zhuang is the Editor-in-Chief of IEEE Transactions on Vehicular Technology, and the Technical Program Symposia Chair of the IEEE Globecom 2011. She is a Fellow of the IEEE, a Fellow of the Canadian Academy of Engineering (CAE), a Fellow of the Engineering Institute of Canada (EIC), and an elected member in the Board of Governors of the IEEE Vehicular Technology Society. She was an IEEE Communications Society Distinguished Lecturer (2008-2011).

Xuemin (Sherman) Shen (M'97-SM'02-F'09) received the B.Sc.(1982) degree from Dalian Maritime University (China) and the M.Sc. (1987) and Ph.D. degrees (1990) from Rutgers University, New Jersey (USA), all in electrical engineering. He is a Professor and University Research Chair, Department of Electrical and Computer Engineering, University of Waterloo, Canada. He was the Associate Chair for Graduate Studies from 2004 to 2008. Dr. Shen's research focuses on resource management in interconnected wireless/wired networks, wireless network security, wireless body area networks, vehicular ad hoc and sensor networks. He is a co-author/editor of six books, and has published more than 600 papers and book chapters in wireless communications and networks, control and filtering. Dr. Shen served as the Technical Program Committee Chair for IEEE VTC'10 Fall, the Symposia Chair for IEEE ICC'10, the Tutorial Chair for IEEE VTC'11 Spring and IEEE ICC'08, the Technical Program Committee Chair for IEEE Globecom'07, the General Co-Chair for Chinacom'07 and QShine'06, the Chair for IEEE Communications Society Technical Committee on Wireless Communications, and P2P Communications and Networking. He also serves/served as the Editor-in-Chief for IEEE Network, Peer-to-Peer Networking and Application, and IET Communications; a Founding Area Editor for IEEE Transactions on Wireless Communications; an Associate Editor for IEEE Transactions on Vehicular Technology, Computer Networks, and ACM/Wireless Networks, etc.; and the Guest Editor for IEEE JSAC, IEEE Wireless Communications, IEEE Communications Magazine, and ACM Mobile Networks and Applications, etc. Dr. Shen received the Excellent Graduate Supervision Award in 2006, and the Outstanding Performance Award in 2004, 2007 and 2010 from the University of Waterloo, the Premier's Research Excellence Award (PREA) in 2003 from the Province of Ontario, Canada, and the Distinguished Performance Award in 2002 and 2007 from the Faculty of Engineering, University of Waterloo. Dr. Shen is a registered Professional Engineer of Ontario, Canada, an IEEE Fellow, an Engineering Institute of Canada Fellow, and a Distinguished Lecturer of IEEE Vehicular Technology Society and Communications Society.